SIMULATION OF AIRBAG IMPACT DYNAMICS FOR MARS LANDING*

M. Salama, G. Davis, C.F. Kuo, T. Rivellini, D. Sabahi

Jet Propulsion Laboratory
California Institute of Technology

Abstract:

The use of airbags to attenuate the impact during landing on Mars is described, with emphasis on simulation of its complex dynamics. A simplified low-order impact simulation model is described, which captures the global dynamics at the expense of neglecting localized effects. Details of the modeling concept are given, along with results of several simulations. Many developmental and flight-like tests were also performed to evaluate performance of the airbag system and to verify the analysis. Results of the tests are discussed. For most parameters, good correlation is obtained between results of analysis and tests.

1. Introduction:

The use of airbags to soften the impact during collision is not new. Aside from their present day use in cars and trucks to protect their passengers at times of collision, the concept was proposed for use in space in the pioneering work of Ross and Layman thirty years ago, [1]. In that reference, the authors studied, designed, fabricated, and tested a prototype inflated spherical-shaped "impact limiter" for a mission that was to deliver a lander on Mars. The mission was never built, and the concept never advanced beyond the prototype, until recently, when the NASA Mars Pathfinder mission became a reality.

In addition to delivering a number of science instruments to the surface of Mars, the Pathfinder mission is intended to demonstrate key low cost technologies for use in future science missions to Mars. Among these technologies is the landing system. Upon entering the Martian atmosphere at about 7000 m/sec, the spacecraft will deploy a series of breaking devices (parachutes and solid rockets) to slow down its speed to less than 20 m/sec as it impacts with the Martian ground. To cushion the science instruments from the landing impact, an airbag system is inflated to surround the lander approximately five seconds before impact. After multiple bounces, the lander/airbags comes to rest, the airbags are deflated and retracted, and the lander opens up its petals to allow a microrover to begin exploration, Fig. (1). Of interest here, is the impact and landing phase. In this paper, we focus on the methodology used to simulate the nonlinear dynamics of lander/airbags landing impact, and how this simulation correlates with developmental and flight-like tests.

2. Lander/Airbag Design Concept:

The lander is 330 kg tetrahedral-shaped, Fig. (1), consisting of four deployable petals, one on each face of the tetrahedron. A microrover and science instruments are mounted on the inside of the petals. Four airbags are tethered to the outside of the four petals by kevlar tendons. Each of the four airbags consists of six spherical-shaped lobes which are merged together to form a single larger volume, Fig. (2a). Tethering of a typical airbag to its petal is accomplished by a set of external tendons (dotted in Fig. 2b) that follow the valleys between the six lobes, and a set of internal tendons that tie the cusp points on the airbags to six hard points on each petal. Internal movement of the pressurization gas between airbags is allowed directly between the bottom airbag and each of the side airbags through $0.5 m^2$ Orifices, but is not allowed direct communication between side airbags.

*This work was performed at the Jet Propulsion Laboratory, California Institute of Technology, under contract with the National Aeronautics and Space Administration.

Keywords: Airbags, landing dynamics, impact, nonlinear dynamics, spacecraft loads

The dynamics of airbag impact attenuation system described above begins with the inflated airbags (with tendons taut) receiving the initial landing impact load upon contact with ground. Then during a relatively complex deformation pattern of the inflated airbags, gas compression and movement between airbags through the venting orifices, and slacking of spaced the initially taut tendons, the loads are attenuated and transferred to the relatively rigid tetrahedral lander. Upon contacting ground, the airbag skin is designed to transfer all of the impact load to the contained pressurized gas and the tendons. By virtue of the gas's much lighter weight over the weight of skin and tendons, it is a more efficient energy absorber, and is therefore relied upon to transfer and attenuate the majority of the impact energy. This is made possible by using ' tendon materials and skin fabrics that are almost inextensible. During impact, the gas compression, healing, and movement through the orifices act as mechanisms for energy transfer as well as for energy attenuation. Further energy transfer and attenuation is contributed by the tendons and skin. Before impact, the undeformed configuration of the inflated airbags is designed such that the inflation pressure keeps the tendons taut, as evenly as possible. During impact, the skin and tendons in the vicinity of ground contact area become slack, the loads are redistributed, and support of the increased gas pressure in the deformed configuration is provided by increased tension in the remaining skin and tendons. Friction between the airbags and Martian ground is a very important energy attenuation mechanism, especially when landing occurs at non-vertical angle of attack on a rocky terrain. I'bus, in addition to their high modulus of elasticity, the tendons and exterior of the skin must have high abrasion and puncture resistance. These requirements are satisfied by a multilayer composite skin fabric.

3. Impact Simulation Model:

When simulating the airbag impact dynamics, one is tempted to construct a high fidelity large deformation finite element model that includes detailed geometry and properties of the lander and airbag tendons, skin fabrics, and gas system. In fact this approach was first attempted using thousands of elastic degrees of freedom in nonlinear finite element codes. But while this type of detailed model could be useful for assessing the localized stresses in the tendons and skin, it had the drawback of requiring enormous time and computing resources to obtain useful results. In addition, numerical conditioning problems seemed to grow with the number of degrees of freedom in the model 3'bus, to complement the above effort, a simplified model was created to capture the global impact dynamics of the system with good fidelity but low computing resources. To this end, a highly reduced 30 degrees of freedom model was constructed using the Automatic Dynamic Analysis Mechanical Systems (ADAMS) software. The modeling primitives in ADAMS provide various ways to connect any collection of rigid bodies by various types of joints, forces and pressure systems that may be defined by a wide range of mathematical expressions and variables. A limited number of the traditional one-dimensional flexible elements such as rods, beams, and spring/dashpots are also available. Matrix and/or matrix/differential equations can be part of the model. As discussed subsequently, these capabilities proved useful in modeling the gas flow among airbags. To a large degree, flexibilities and nonlinearities in the system are modeled by functional expressions of forces and pressures., and to a lesser degree by finite elements.

The 30 degree of freedom model consists of one central rigid body representing the lander with six degrees of freedom, surrounded by four rigid bodies each having six degrees of freedom to represent each of the airbags. The tetrahedral lander is defined geometrically by twelve markers, Fig (3), to which tendons of all four airbags are connected Each of the four airbags is about 17.5 kg , and is geometrically defined by eleven markers: one at the center of each of the six lobes (labeled "A" in Fig 2a), four markers at the cusp points (labeled "B" in Fig 2b) to which the tendons join together, and one marker at the geometric center of each bag , to which the mass and inertia properties of a bag is referenced Markers located on the same rigid body move together rigidly, while ones located on different rigid bodies deform relative to each other depending on the. system of forces, constraints, and flexible connections that join them. in this context, the six spherical lobes belonging to the same airbag do not deform relative to each other, but deform relative to other lobes in the system.

Before impact, the inflated system of airbags is in a state of quasi-static equilibrium, in which the inflation pressure is supported by the airbag skin being tightly tethered to faces of the tetrahedral lander by a system of tendons. The airbag skin itself is not modeled explicitly, but is substituted by the pressure forces within This is simulated by a combination of (a) resultant pressure forces acting outward at the center of each of the 24 lobes, (b) resultant pressure forces acting inward and normal to the faces of the tetrahedral

lander, (c) pairs of bag-to-bag pressure resultants applied at contacting lobes of different airbags in directions normal 10 the contact surfaces, and (d) a set of self-cquilibrat i ng tendon forces.

By definition, each tendon joining markers r and s carries tension form only, $T(t)_{rs}$, the magnitude of which is a function of the instantaneous change in length $(l(t)_{rs} - l_0)$ from the unstressed state

$$F_{rs} = EA(-1 + 1,' /1.), \quad l_{rs} > 10,$$
$$= 0 \text{ otherwise} \qquad (1)$$

On the other hand, the pressure resultants are function of the instantaneous contact surface- areas and instantaneous pressure, both of which are derived from local gas movement and changes in geometry. Thus, if $p(t)_m$ and $p(t)_n$ is the instantaneous pressures in airbags m and n (each of which have six lot < s), and d_{ij} (f) is the instantaneous distance between the centers of lobes i and j, which belong to airbags m and n, respectively, then the contact force between the two lobes is

$$F_{ij} = \pi (R^2 - d_{ij}(t)^2)(p(t)_m + p(t)_n)/8 \qquad (2)$$

Equation (2) idealizes the region of contact by a circular area defining the intersection between two overlapping spherical lobes with radius R

All four airbags start initially with equal inflation pressures before impact. Subsequent pressure changes during impact arc duc to gas flow through the internal orifices between bags, and due to volume changes as the bags arc deformed. The gas is assumed perfect. Its flow through the venting orifices can be sonic or subsonic, depending upon the ratio of the pressures downstream and upstream. For subsonic flow, the rate of mass of gas flowing through the orifice between airbags m and n is [2] :

$$dm_{mn}/dt = kA_v P_d [(1/GT)(2\gamma/(\gamma - 1))(P_u/)'\#)^{\cdots} \times ((P^{\cdots}/P_d)^{(\gamma-1)/\gamma} - 1)]^{0.5} \qquad (3)$$

where: P_o = initial pressure, P_u = upstream pressure, P_d = downstream pressure, A_v = venting orifice area, y = specific heat ratio, G = gas constant, k = orifice coefficient (Ref. [3]), and 7 = gas temperature

Similarly, for sonic flow:

$$dm_{mn}/dt = kA_v P_d [(1/GT)(2\gamma/(\gamma + 1))^{(\gamma+1)/(\gamma-1)} \times (P_u/P_0)^{(\gamma+1)/\gamma}]^{0.5} \qquad (4)$$

Integration of three nonlinear equations as indicated by (3) 01 (4) for the gas flow between bags (1,2) , (1,3) , and (1,4) is done numerically at each discrete time point in the simulation to calculate the mass of gas transferred between airbags. Assuming constant density, this is then used to compute the change in volume $\Delta V(t)_f$ in each airbag duc to gas flow.

in addition to gas flow, volumetric changes $\Delta V(t)_v$ result from crushing of the bottom airbag as it contacts ground, and from the side airbags being squeezed against each other, As two spherical-shaped lobes i and j belonging to two different airbags arc compressed together to a center-to-center distance $d(t)_{ij}$ a volume change in each lobe is idealized by the loss of the over la pping volume of two spheres of radius R:

$$(\Delta V_{ij})_v = (\pi/3)(R - d_{ij}/2)^2(2R + d_{ij}/2), \quad R > d_{ij}/2$$
$$= 0 \quad \text{otherwise} \qquad (5)$$

Similarly, when lobe i is compressed against ground during impact, the change in volume of this lobe is:

$$(\Delta V_{ig})_v = (\pi/3)(R - d_{ig})^2(2R + d_{ig}), \quad R > d_{ig}$$
$$= \text{O otherwise} \qquad (6)$$

where $d(t)_{ig}$ is the distance between the center of lobe i and ground, along the normal to ground, The total change in volume for airbag m is simply the sum from all of the aforementioned effects:

$$\Delta V_m(t) = [(\sum_i \Delta V_i(t))_v + (\Delta V(t))_f]_m \qquad (7)$$

The corresponding pressure is found from:

$$P_m(t) = P_0[V_0/(V_0 - \Delta V_m(t))]^{\gamma} \qquad (8)$$

Landing is simulated by monitoring all 24 distance-to-ground landing vectors $d(t)_{ig}$ i = 1,...,24 as function of time. Each vector is directed along the normal to ground between the center of each of the 24 lobes and ground If the length of one (or more) of the normals $d(t)_{ig}$ becomes less than the lobe radius R,

then that lobe(s) has contacted ground At which time, components of ground reaction $R(t)_{in}$, $R(t)_{ig}$ in directions normal and parallel to ground, are immediately applied to the lobe(s) in contact with ground. The magnitude of the components of ground reaction depend on the instantaneous contacting surface area, instantaneous airbag pressure differential $P(t)_i$, and the coefficient of ground friction

$$R_{in} = P_i \times A_{ig}$$
$$R_{ig} = R_{in} \times friction\ coeff. \qquad (9)$$

where, similar to Eq.(2) $A_{ig} = \pi\delta_i(2R - \delta_i)$ is the contact area, and $\delta_i = R - d_{ig}$ is the corresponding stroke.

4. Drop' Tests:

A comprehensive test program was carried out from the initial design phase to the final qualification of the flight airbag landing system. Two series of these tests, hereafter referred to as .38 scale and flight system drop tests, are described next. Their objectives were to (a) establish correlation between the analysis and test results, (b) evaluate the airbag performance as a function of a number of design parameters, and (c) verify survivability of the design in a realistic simulation of the Martian conditions.

A, .38 Scale Tests: This series of tests were developmental in nature and emphasized the first two objectives. A number of deviations from the expected design conditions were implemented for ease of testing and to allow greater control over test parameters 1 or example, the airbag/lander system was simulated by a 0.38 scale model that preserved most of the attributes of the full scale design [2], with the 0.38 ratio being the ratio between Mars and Earth gravity. Most importantly, rather than dropping the airbag/lander model to ground, the model was kept stationary and an appropriately scaled mass of 27.66 kg impact plate (representing ground) was accelerated to hit the airbags at a prescribed angle. Several test parameters were Varied that included the magnitude and or it-l ration of the impact velocity, venting scheme and size of venting orifices between airbags. These parameters have considerable influence on the landing dynamics and degree of impact attenuation. Test measurements included the velocity at impact, displacement stroke of the impacted airbag, pressure and temperature profiles of all airbags, acceleration profile of the impacting plate, and the forces in selected tendons,

B. **Flight System Drop Tests**: These tests simulate the Martian landing conditions of the full scale airbag/lander system. To this end, verifying survivability of the design and its performance was of primary importance, especially for the airbag skin design (bladder and fabric). Results of these tests are intended to guide further design modifications and subsequent testing, Relying completely on tests to verify the integrity of the airbag skin was a result of the absence of credible and practical analytical tools that can predict stresses there to a reasonable accuracy. This is so, partly because of the numerical difficulties discussed in Section 3, and mostly because the actual landing conditions on Mars surface, will most likely encounter a rocky terrain. Specific configurations of the rocks - such as size, distribution, and sharpness - will to a large extent determine the local maximum stresses in the skin. Such information is lacking in a deterministic sense, thereby making analytical predictions of design stresses in the airbag skin impractical.

The test configuration, Fig (4), consisted of the prototype airbag system attached in flight like fashion to a full scale engineering model of the lander. The airbags were instrumented with thermocouples and pressure transducers to measure airbag thermodynamic performance parameters. in addition, a selected set of tendons connecting one of the aid-rags to the lander were instrumented with inline load cells to measure the tendon forces, and the lander was instrumented with accelerometers to record its six degrees of freedom rigid body kinematics throughout the tests. All data was recorded on a portable acquisition system mounted inside the moving lander. The combined airbag/lander assembly was suspended from the top of the environmental test chamber, then allowed to drop onto either a horizontal surface or a platform inclined 60" with a simulated rock field. The 60" incline simulates the design landing condition of 30° with respect to the Martian surface, and the rock field simulates the actual Martian surface rock distribution based on the Viking lander data. The range of velocity magnitude and orientation at impact used in these tests were guided by a recent study [4], in which Monte Carlo simulations of I he entire sequence of entry, descent, and landing was used to determine probability distributions for the terminal landing velocity and orientation of the airbag/lander .q'stern Fifteen drop tests were performed under various combination of conditions,

wherein the impact velocity ranged from 15 m/s to 28 m/s at either horizontal or 60" incline, the rock sizes were either 0 (no rocks), 0.3 m, or 0.5 m, and the initial inflation pressure in the airbags was set at values between 0.89 and 1.5 psia. All tests took place at ambient chamber pressure of approximately 5 torr, Martian surface ambient condition.

5. Analysis and Test Results:

Predicting the worst case landing conditions and how these affect design of the science instruments on-board is of primary importance. For this purpose, numerical simulations were carried out with various combination of design parameter values such as initial airbag pressure, writing orifice areas, impact velocity magnitude and direction, as well as assumed values for damping - both internal in the system and external to the system (clue to friction between the airbag, lander and Martian ground). Furthermore, since the simulation model contains many idealizations, it is important to validate the simulation approach and assumptions by comparison with selected test conditions. This was done first by simulating the .38 scale test configuration discussed in Section 4A and subsequently by simulating the flight system drop test of Section 4B.

A. .38 **Scale Correlation: Two** representative cases are selected here from among several ones used for analysis - test correlation. In the first case, the bottom airbag was flatly impacted by the plate at 13.5 m/s. In the second case the lander was rotated 70.5° so that at impact (at -15.0 m/s velocity) occurs at three lobes belonging to three different airbags that share a common tetrahedral vertex. This is referred to as oblique impact. Tables 1 and 2 compare the analytically predicted steady state and peak responses with their corresponding test values for the two cases above. Comparison between time histories is further illustrated for the **first case (flat impact)** in figs (5,6) for the acceleration and pressure time history for the impacted airbag, and in Fig (7) for pressure time history in a typical side airbag. From all cases considered, including those in Tables 1,2, the peak acceleration, airbag pressure, and the steady state tendon loads agree quite well (within 5%), while the rebound velocity of the impact plate and the airbag deformation (stroke) compare less favorably (<20%). The peak dynamic tendon loads showed the least agreement (~200%) - with the analysis being conservative. This may be expected, since the highly compliant airbag skin at the junction of a group of tendons was not modeled elastically (modeled as infinitely stiff).

Table 1:.38 Scale Bottom Airbag Impact Correlation

Response	Test	Analysis
Velocity (m/s):Impact/Rebound	13.5 / 7.1	13.5 / 10.88
Peak Acceleration (g)	39	40.8
Stroke (m)	0.37	0,29
Pressure (P1,kPa):Initial/Peak	8.1 /11.0	8.1 /11.4
Pressure (P2-P4,kPa):Initial/Peak	8.119.2	8.119.05
Tendon Force (F1,N):Initial/Peak	400/520	540/1293
Tendon Force (F2,N):Initial/Peak	3001450	3081750
Tendon Force (F4,N)Initial/Peak	400/480	410/480

Table 2:.38 Scale Oblique Impact Correlation

Response	Test	Analysis
Velocity (m/s):Impact/Rebound	14.9 / 8.8	14.9 / 12.4
Peak Acceleration (g)	37	52
Stroke (m)	0.5	0.39
Pressure (P1,kPa):Initial/Peak	8.019.5	8,418.8
Pressure (P2,kPa):Initial/Peak	8.0110.0	8.419.7
Pressure (P3,P4,kPa):Initial/Peak	8.0 / 10.1	8.419.9
Tendon Force (F1,N):Initial/Peak	400 / 450	570 / 1250
Tendon Force (F2,N):Initial/Peak	203/250	310/800
Tendon Force (F4,N):Initial/Peak	320/1000	430 / 2920

B. Flight System Correlation: Full scale lander/airbag system in flight like conditions were tested and numerically simulated for landing on a flat smooth surface (Fig 8) and on rocky inclined slopes (Fig 9). Comparison of analysis and test results of two landing cases on flat surface are shown in Tables 3 and 4. In Table 3, the system is dropped vertically so that it lands upright on the bottom airbag at an impact velocity of 15 m/s. In Table 4, the system is dropped also vertically, but is rotated such that it lands on one of the side airbags at an impact velocity of 20 m/s. Aside from the impact speed, the main difference between the above two cases is the venting path from the impacted airbag to the other three airbags. Direct venting is allowed only through three orifices between the bottom airbag and each of the side ones. No direct venting is allowed between side airbags. This influences how the airbag pressure and other response parameters change during impact

Table 3: Flight Test Correlation, (Bottom bag landing)

Response	Test	Analysis
Velocity (m/s):Impact/Rebound	15. I 13.53	15 / 13 5
Peak Acceleration (g)	26.3	26 31
Stroke (m)	0.79	0 65
Pressure (P4,kPa):Initial/Peak	10.62/1341	10.62 / 13 5
Pressure (PI -P3,kPa):Initial/Peak	10.62/120	10.62 / 12 5
Peak Tendon Force (F I,N)	2735	30 5
Peak Tendon Force (F2,N)	2558	32 4
Peak Tendon Force (F3,N)	3760	6140
Peak Tendon Force (F4,N)	979	26 8
Peak Tendon Force (F5,N)	4276	75 7
Peak Tendon Force (F6,N)	890	24 6

Table 4: Flight Test Correlation, (Side bag landing)

Response	Test	Analysis
Velocity (m/s):Impact/Rebound	'p9x31171	20 / 18 1
Peak Acceleration (g)	38.25	3
Stroke (m)	1.12	0 91
Pressure (PI ,kPa):Initial/Peak	10.43 I 17.58	10 43 / 17 07
Pressure (P4,kPa):Initial/Peak	1043/15 16	10 43 / 13 43
Pressure (P2-P3,kPa):Initial/Peak	10,43 / 1338	10 43 / 13 0(

An example of test results of airbag drops on an inclined rocky surface in Fig 9 is given in Fig 10. Considering the geometric center of the ai rbag/under system, Figs 10 (a, b, c) respectively, show the trajectory, velocity, and acceleration history during a typical drop. This test was not simulated by analysis due to the random nature of rock landing and the uncertainty in quantifying the coefficient of friction between the airbags and the rocky field

6. (conclusions:

Airbag landing is a nonlinear contact problem 'I he dynamic response is influenced in a relatively complex manner by a number of interacting, parameters. Ideally, detailed mathematical structural models with thousands of degrees of freedom are constructed to capture details of the dynamic response. For the present problem, this approach was not very beneficial. Instead, and at the expense of gross inaccuracies in localized response quantities such as stresses, global dynamics of the airbag landing is captured by a simplified 30 degrees of freedom simulation model. In part, this is achieved by functional representation of the nonlinear relationships between the problem parameters. An example is the relationship between parameters of the gas dynamics and the structural stiffness and deformation of the airbag during impact, Success of the approach is evidenced by the good agreement between analysis and test results.

Acknowledgment:

The .38 scale tests were performed at Sandia National Laboratories, Albuquerque, NM, and the flight-like airbag system tests were performed at the Space Power Facility at NASA Lewis Research Center's Plum Brook Station. In collaboration with 1 LC Dover, Inc. The efforts and cooperation of all involved are gratefully acknowledged.

References:

1. Ross, R G., Layman, W. E.: "The Design and Testing of an Inflated Sphere impact Limiter", JPL Technical Report No. 32- 1037, December 1969.

2. Wave, D. E, Cole, J. K., Rivellini, T. P.: "Mars Pathfinder Airbag Impact Attenuation System", paper presented at the AIAA Aerodynamics Decelerator Conference, May 1995.

3. Perry, J. A., Jr.: "Critical Flow Through Sharp Edged Ori frees," Transactions of the American Society of Mechanical Engineers, October 1949, pi). 757-764.

4. Smith, K. S., Peng, C-Y., and Behboud, A., "Multibody Dynamic Simulation of Mars Pathfinder Entry, Descent, and landing", Jet Propulsion Laboratory document No. D-13298, April 1995,

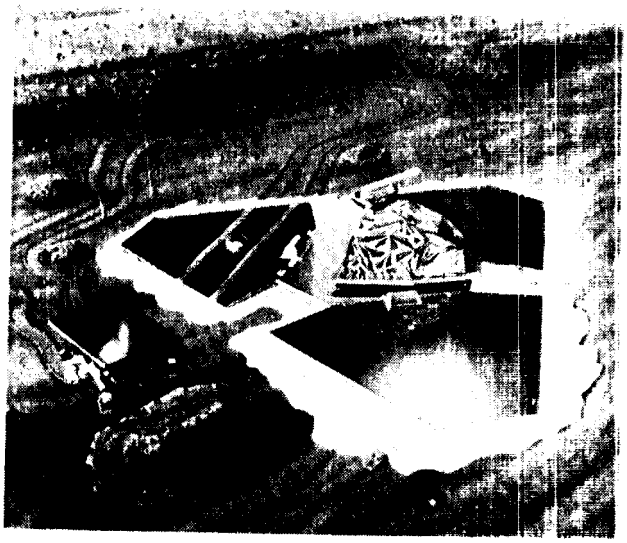

Fig 1: Mars Pathfinder Landing Cone-cj,l

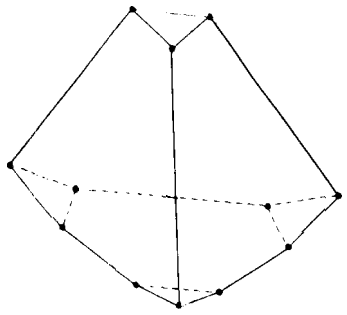

Fig 3: Tetrahedral Lander Model

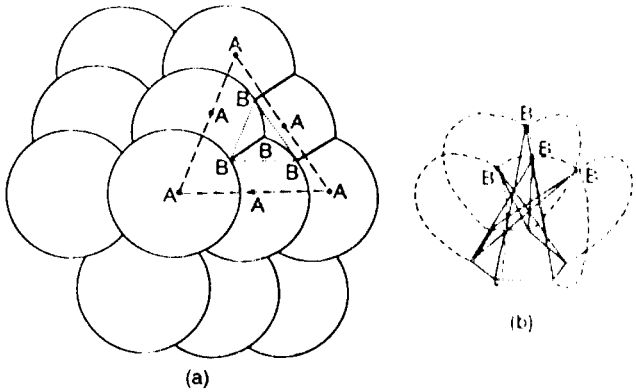

Fig 2: Six-Lobe Airbag Configuration,
(a) Six Lobes, (b) Tendons

Fig 4: Flight Prototype Airbag/Lander System

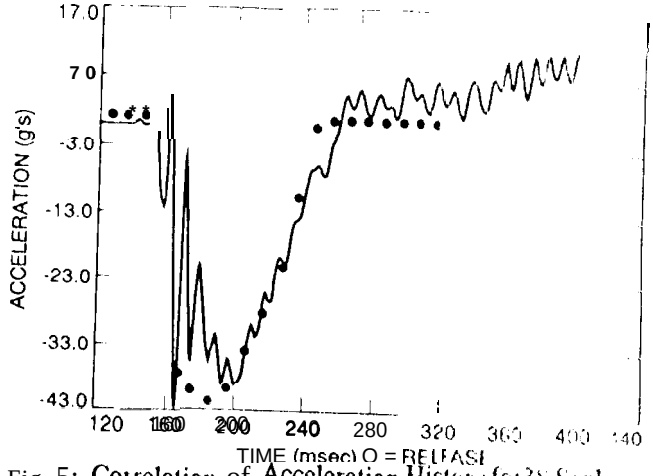

Fig 5: Correlation of Acceleration History for 38 Scale Test (solid line).

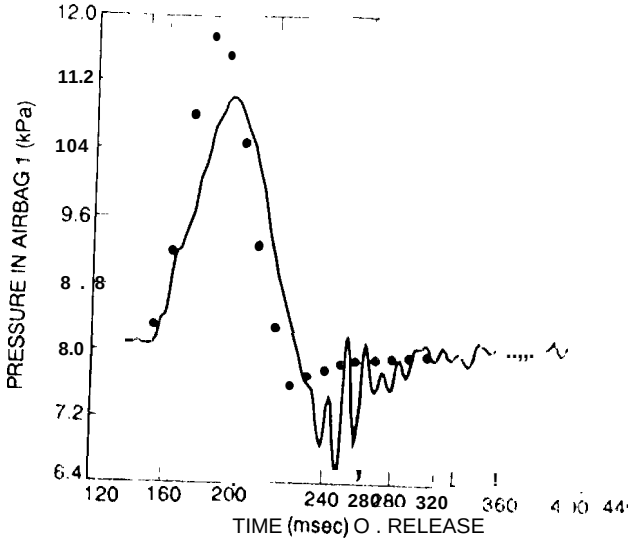

Fig 6: Correlation of Pressure History for Impacted Airbag in .38 Scale Test.

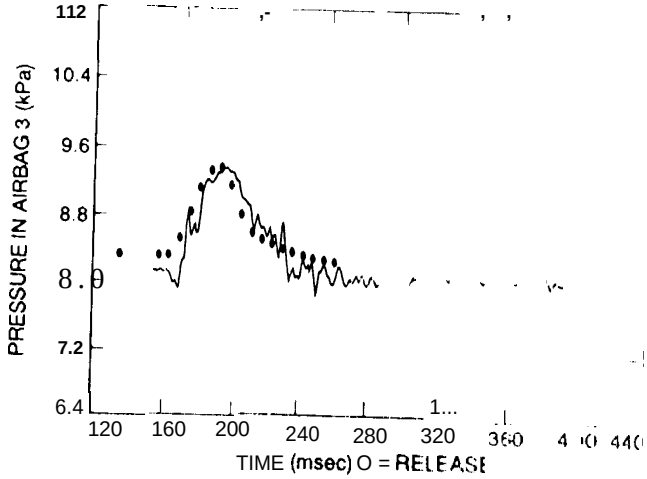

Fig 7: Correlation of Pressure History for Side Airbag in .38 Scale Test.

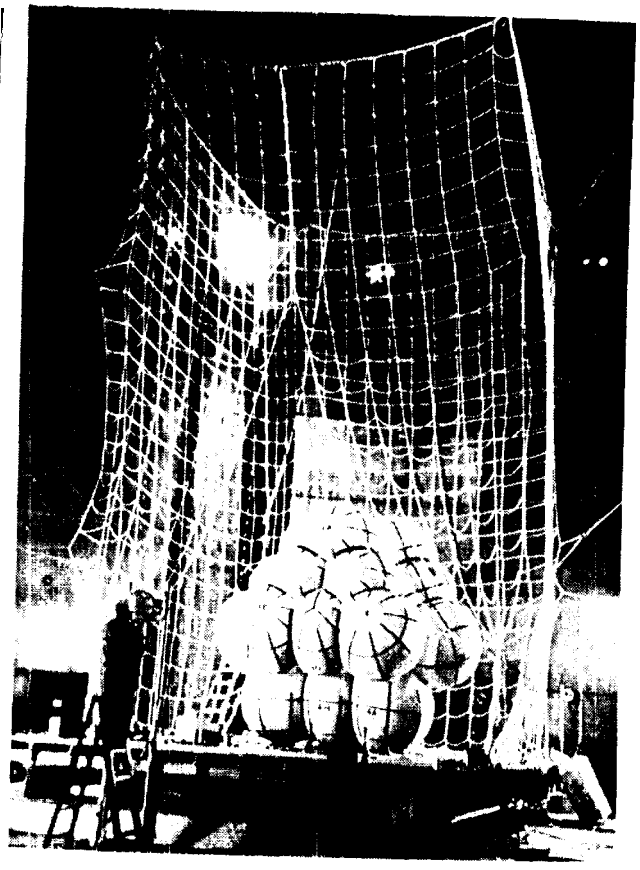

Fig 8: Flight Prototype System Landing on Flat Surface

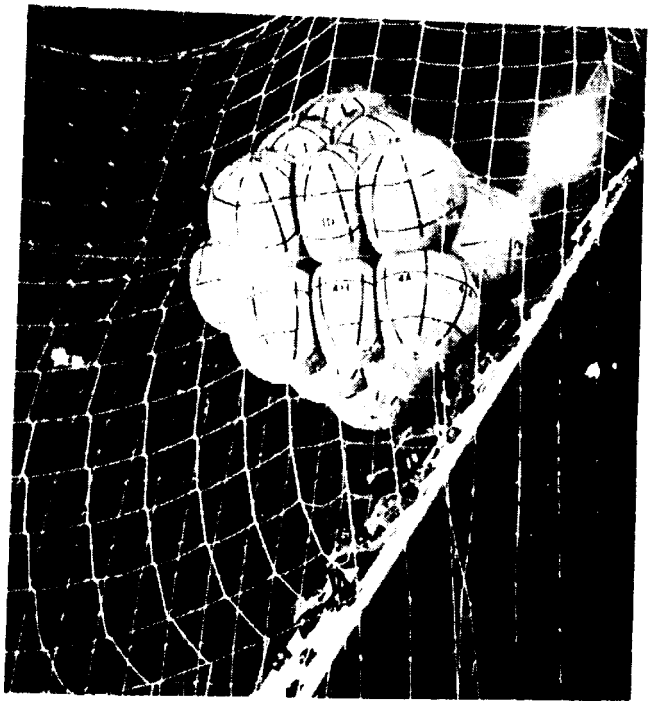

Fig 9: Flight Prototype System Landing on Rocky Incline

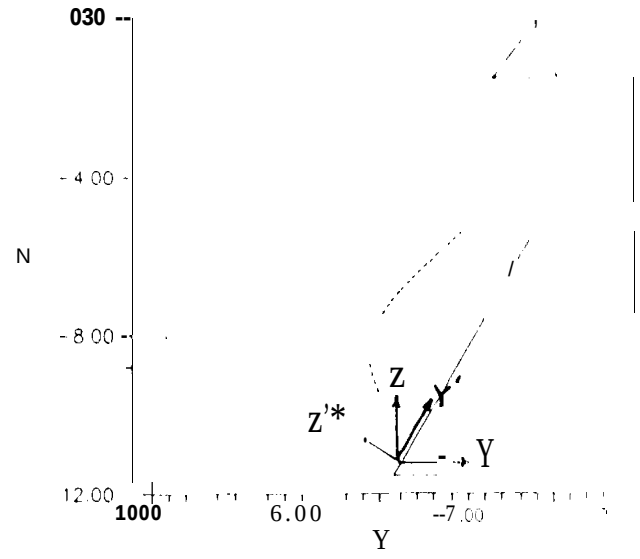

Fig 10: Results of Landing on Inclined **Rocky Field**
(a) Trajectory of Centroid, (b) Velocity of Centroid,
(c) Acceleration of Centroid.